JPET Fast Forward. Published on October 25, 2020 as DOI: 10.1124/jpet.120.000121
This article has not been copyedited and formatted. The final version may differ from this version.

K_{ATP} Channel Openers Inhibit Lymphatic Contractions and Lymph Flow as a Possible Mechanism of Peripheral Edema

Brittney R. Garner, Amanda J. Stolarz, Daniel Stuckey, Mustafa Sarimollaoglu, Yunmeng Liu, Philip T. Palade, Nancy J. Rusch, and Shengyu Mu

Affiliations:

Department of Pharmacology and Toxicology, College of Medicine, University of Arkansas for Medical Sciences, Little Rock, AR 72205 (BRG, AJS, DS, YL, PTP, NJR, SM)

Department of Pharmaceutical Sciences, College of Pharmacy, University of Arkansas for Medical Sciences, Little Rock, AR 72205 (AJS)

Arkansas Nanomedicine Center, College of Medicine, University of Arkansas for Medical Sciences, Little Rock, AR 72205 (MS)

Running Title Page: K_{ATP} Channel Openers Inhibit Lymphatic Contractions and Flow

Corresponding Author:

Shengyu Mu, MD, PhD

Assistant Professor

Department of Pharmacology and Toxicology

University of Arkansas for Medical Sciences

4301 W. Markham Street, #611

Little Rock, AR 72205-7199

Phone: (501) 686 5510

Fax: (501) 686 5521

smu@uams.edu

Downloaded from jpet.aspetjournals.org at ASPET Journals on April 18, 2024

JPET Fast Forward. Published on October 25, 2020 as DOI: 10.1124/jpet.120.000121
This article has not been copyedited and formatted. The final version may differ from this version.

Number of text pages: 16

Number of tables: 3 + 2 supplemental tables

Number of figures: 8 + 1 supplemental figure

Number of references: 51

Number of words in *Abstract*: 235

Number of words in *Introduction*: 742

Number of words in *Discussion*: 1,434

Nonstandard Abbreviations: K_{ATP} channel, ATP-sensitive potassium channel; KCO, K_{ATP} channel opener; LVs, lymph vessels; LMCs, lymphatic muscle cells; EDD, end diastolic diameter; ESD, end systolic diameter; SMC, smooth muscle cell.

Recommended Section Assignment: Cardiovascular

Downloaded from jpet.aspetjournals.org at ASPET Journals on April 18, 2024

JPET Fast Forward. Published on October 25, 2020 as DOI: 10.1124/jpet.120.000121
This article has not been copyedited and formatted. The final version may differ from this version.

Abstract

Pharmacological openers of adenosine triphosphate-sensitive K^+ (K_{ATP}) channels are effective antihypertensive agents, but off-target effects, including severe peripheral edema limit their clinical usefulness. It is presumed that the arterial dilation induced by K_{ATP} channel openers (KCOs) increases capillary pressure to promote filtration edema. However, K_{ATP} channels also are expressed by lymphatic muscle cells (LMCs), raising the possibility that KCOs also attenuate lymph flow to increase interstitial fluid. The present study explored the effect of KCOs on lymphatic contractile function and lymph flow. In isolated rat mesenteric lymph vessels (LVs), the prototypic K_{ATP} channel opener cromakalim (0.01–3 μmol/L) progressively inhibited rhythmic contractions and calculated intraluminal flow. Minoxidil sulfate and diazoxide (0.01–100 μmol/L) had similar effects at clinically relevant plasma concentrations. High speed in-vivo imaging of the rat mesenteric lymphatic circulation revealed that superfusion of LVs with cromakalim and minoxidil sulfate (0.01-10 μmol/L) maximally decreased lymph flow *in vivo* by 38.4% and 27.4%, respectively. Real-time PCR and flow cytometry identified the abundant K_{ATP} channel subunits in LMCs as the pore-forming Kir6.1/6.2 and regulatory SUR2 subunits. Patch-clamp studies detected cromakalim-elicited unitary K^+ currents in cell-attached patches of LMCs with a single-channel conductance of 46.4 pS, a property consistent with Kir6.1/6.2 tetrameric channels. Addition of minoxidil sulfate and diazoxide elicited unitary currents of similar amplitude. Collectively, our findings indicate that KCOs attenuate lymph flow at clinically relevant plasma concentrations as a potential contributing mechanism to peripheral edema.

Significance Statement

Potassium channel openers (KCOs) are potent antihypertensive medications, but off-target effects including severe peripheral edema limit their clinical use. Here, we demonstrate that KCOs impair the rhythmic contractions of lymph vessels and attenuate lymph flow, which may promote edema formation. Our finding that the K_{ATP} channels in lymphatic muscle cells may be unique from their counterparts in

Downloaded from jpet.aspetjournals.org at ASPET Journals on April 18, 2024

JPET Fast Forward. Published on October 25, 2020 as DOI: 10.1124/jpet.120.000121
This article has not been copyedited and formatted. The final version may differ from this version.

arterial muscle implies that designing arterial-selective KCOs may avoid activation of lymphatic K_{ATP} channels and peripheral edema.

Introduction

Adenosine triphosphate-sensitive K^+ (K_{ATP}) channels are metabolically sensitive ion channels in the plasma membrane, which open in response to low intracellular concentrations of ATP and other metabolic challenges. The opening of K_{ATP} channels mediates K^+ efflux, membrane hyperpolarization, closure of voltage-gated calcium channels, and reduced excitation of many cell types (Mannhold, 2004; Foster and Coetzee, 2016). In arterial smooth muscle cells (SMCs), the pharmacological activation of K_{ATP} channels exerts powerful vasodilator and blood pressure lowering effects. Indeed, pharmacologic openers of K_{ATP} channels (KCOs) were administered as antihypertensive agents prior to understanding their mechanism of action. Minoxidil was approved in 1971 for the treatment of hypertension (Bryan, 2011) followed by the introduction of diazoxide in 1976 (Lexicomp, 2020). Although the prototypic KCO, cromakalim, was synthesized from a β-blocker skeleton in the 1980s (Mannhold, 2004), it was not until 1983 that Noma and colleagues discovered the K_{ATP} channel in cardiomyocytes (Noma, 1983). Subsequently, new structural families of KCOs were synthesized but only minoxidil and diazoxide were ever approved for clinical use in the United States. Minoxidil is used for hypertensive emergencies in patients resistant to standard antihypertensive medications. Diazoxide was developed as an antihypertensive medication, but has evolved into a valuable drug for treating persistent hyperinsulinism (Welters *et al.*, 2015).

Although the KCOs are potent antihypertensive agents (Nichols *et al.*, 2013; Rubaiy, 2016), they are not drugs of choice to treat chronic hypertension due to potentially severe side effects, including peripheral edema, which manifests as fluid retention and gross swelling of the feet and/or legs (Sica, 2004; Nichols *et al.*, 2013). A common presumption is that peripheral edema results when KCOs preferentially dilate arteries compared to veins, resulting in elevated capillary pressure and movement of intravascular fluid into tissues to establish filtration edema (Sica, 2003; Weir, 2003). Indeed, the

Downloaded from jpet.aspetjournals.org at ASPET Journals on April 18, 2024

JPET Fast Forward. Published on October 25, 2020 as DOI: 10.1124/jpet.120.000121
This article has not been copyedited and formatted. The final version may differ from this version.

molecular composition and pharmacology of K_{ATP} channels in arterial SMCs and their response to KCOs is well defined. Arterial K_{ATP} channels primarily are composed of four pore-forming Kir6.1 subunits physically associated with four regulatory sulfonylurea receptor isoform 2B subunits (SUR2B) (Shi *et al.*, 2012; Monique N. Foster and Coetzee, 2016; Rubaiy, 2016). The SUR2B subunit contains binding domains for KCOs, which when occupied, antagonize ATP-mediated pore inhibition as the basis for pharmacological activation of K_{ATP} channels and vasodilation (Mannhold, 2004; Foster and Coetzee, 2016).

In contrast to the arterial circulation, only a limited number of studies have described the effect of KCOs on the lymphatic circulation. Interestingly, lymph vessels are composed of "hybrid" lymphatic muscle cells (LMCs), which share functional properties with smooth and striated muscle cells, and express smooth, cardiac and skeletal muscle biomarkers (Muthuchamy *et al.*, 2003). Similar to cardiac myocytes, collecting lymph vessels exhibit rhythmic contractions. In the lymphatic circulation, these contractions "pump" fluid from the extracellular space to the central venous ducts to prevent the formation of edema (Gashev, 2002; Choi *et al.*, 2012; Nipper and Dixon, 2013; Mortimer and Rockson, 2014). In guinea pig mesenteric lymphatics, micromolar concentrations of cromakalim inhibit the rhythmic contractions of collecting lymph vessels (Mathias and von der Weid, 2013), implying that KCOs may impair lymph flow. Similarly, KCOs can abolish the rhythmic contractions of isolated human mesenteric lymph vessels (Telinius *et al.*, 2014). However, whether KCOs inhibit the rhythmic contractions of collecting lymph vessels at clinically achievable plasma concentrations is unclear and the effect of KCOs on lymph flow in vivo has not been reported to our knowledge. Finally, although transcripts encoding the K_{ATP} channel Kir6.1 and SUR2B subunits were reported in guinea pig mesenteric LVs (Mathias and von der Weid, 2013), the identity of the protein subunits that co-assemble to form K_{ATP} channels in LMCs also is unclear.

The goal of the present study was to define the impact of the prototypic KCO, cromakalim, and of clinically relevant concentrations of minoxidil and diazoxide, on the rhythmic contractile activity of

Downloaded from jpet.aspetjournals.org at ASPET Journals on April 18, 2024

JPET Fast Forward. Published on October 25, 2020 as DOI: 10.1124/jpet.120.000121
This article has not been copyedited and formatted. The final version may differ from this version.

isolated rat mesenteric LVs and evaluate whether KCOs impair lymph flow in vivo. A final set of studies used flow cytometry and patch-clamp recordings to identify the subunit composition of functional K_{ATP} channels in single LMCs. Our findings indicate that the rhythmic contractions of rat mesenteric LVs and lymph flow in vivo are impaired by KCOs at concentrations associated with their therapeutic actions. Furthermore, the K_{ATP} channels in LMCs may be structurally distinct from their counterparts in arterial SMCs, implying that differential targeting of arterial versus lymphatic K_{ATP} channels by KCOs may represent one strategy to avoid peripheral edema while retaining powerful blood pressure-lowering effects.

Materials and Methods

Animals

Animals used in experiments were housed in the Division of Laboratory Animal Medicine (DLAM) at the University of Arkansas for Medical Sciences. Animal use protocols (#3672 & #3923) were approved by the Institutional Animal Care and Use Committee under the provisions of the National Institutes of Health guidelines. For all *ex vivo* studies, LVs were obtained from 9 to 13 week-old male Sprague-Dawley rats ordered from Envigo (Indianapolis, IN, USA). Rats were anaesthetized using 2.5% isoflurane with pure oxygen at a flow rate of 3 liters per minute (L/min) for 5 minutes, then euthanized by decapitation. For the purposes of imaging LVs *in vivo,* 5 to 7 week-old male Sprague-Dawley rats from the same vendor were used to minimize mesenteric fat. At the completion of *in vivo* experiments, rats were exsanguinated via cardiac puncture.

Diameter Measurements

Mesenteric LVs

After sacrifice, the rat mesentery was dissected free and placed in a beaker of cold physiological saline solution (PSS) consisting of (in mmol/L): 119 NaCl, 24 $NaHCO_3$, 5.5 glucose, 4.7 KCl, 1.6 $CaCl_2$, 1.17 NaH_2PO_4, 1.17 $MgSO_4$, and 0.026 EDTA. Subsequently, the mesentery was transferred to a silicone-based dissection tray filled with cold PSS. Mesenteric loops were exposed and stabilized by

Downloaded from jpet.aspetjournals.org at ASPET Journals on April 18, 2024

JPET Fast Forward. Published on October 25, 2020 as DOI: 10.1124/jpet.120.000121
This article has not been copyedited and formatted. The final version may differ from this version.

insect pins to allow the dissection of second order LVs from connective and adipose tissue. A single LV was then transferred to a Living Systems perfusion chamber (Living Systems Instrumentation, Burlington, VT, USA) containing PSS at 37˚C with 7% CO_2 bubbling to maintain a pH of 7.4. The LV was cannulated with glass micropipettes (75-100 µm; Living Systems Instrumentation, Burlington, VT, USA) and perfused with PSS in the distal to proximal direction at an intraluminal pressure of 4 to 5 mm Hg. The vessel was allowed to equilibrate for 45 minutes or until rhythmic contractions were stable. Then concentration-dependent diameter responses to KCOs or corresponding solvent were recorded at a sampling rate of 3 frames/second using DMTvas edge-detection software (IonOptix Corporation, Westwood, MA, USA). The KCOs included cromakalim (0.01 to 3 µmol/L; quarter-log units), minoxidil sulfate (0.01 to 100 µmol/L; half-log units) and diazoxide (0.01 to 100 µmol/L; half-log units). Origin 9.1 software (OriginLab Corporation, Northampton, MA, USA) was used to analyze the following contractile parameters: end diastolic diameter (EDD), end systolic diameter (ESD), frequency of contraction, and amplitude of contraction. Flow per unit length in a single lymph vessel was calculated using the equation: $\pi/4(EDD^2-ESD^2)F$, as previously described (Stolarz *et al.*, 2019).

High-Speed *In Vivo* Microscopy

Rats were fasted overnight and anesthetized using 2.5% isoflurane in 1.5 L/min oxygen. A midline abdominal incision was made and a single loop of mesentery was pulled out and placed in a customized heated (37°C) chamber filled with HEPES-PSS consisting of (in mmol/L): 119 NaCl, 4.7 KCl, 1.17 $MgSO_4$, 1.6 $CaCl_2$, 24 $NaHCO_3$, 0.026 EDTA, 1.17 NaH_2PO_4, 5.5 glucose and 5.8 HEPES); pH was titrated to 7.4 using NaOH. A single LV was visualized and increasing concentrations of cromakalim or minoxidil sulfate (0.01 to 10 µmol/L; log units) were added to the superfusate bathing the mesentery for 15 minutes at each drug concentration. Customized software, developed in collaboration with our institution's Nanomedicine Center, was used to track individual lymph cells in flow as described earlier in detail (Sarimollaoglu *et al.*, 2018; Stolarz *et al.*, 2019). Using these data files, flow velocity and positive volumetric flow were calculated to evaluate the effect of KCOs on lymph flow *in vivo*.

Real-Time PCR

Downloaded from jpet.aspetjournals.org at ASPET Journals on April 18, 2024

JPET Fast Forward. Published on October 25, 2020 as DOI: 10.1124/jpet.120.000121
This article has not been copyedited and formatted. The final version may differ from this version.

The entire rat mesentery was pinned in a dissecting tray filled with cold PSS and first to third -order mesenteric LVs were dissected free during a 2-hour interval and immediately placed in a safe-lock tube containing 600 µl of RNeasy Lysis Buffer (RLT) solution (Qiagen, Hilden, Germany) and 1% β-mercaptoethanol. After addition of 200 mg of 0.5-mm stainless steel bullets (Next Advance, Troy, NY, USA), the LVs were homogenized at speed 9 in a Next Advance bullet blender (Next Advance, Troy, NY, USA) for 2 minutes, then after a 2-minute interval to allow for cooling, homogenized for an additional 2 minutes. Total RNA was isolated using the Qiagen RNeasy Plus Mini Kit (Hilden, Germany) according to commercial instructions and stored at -80°C.

Invitrogen's SuperScript™ III Reverse Transcriptase kit was used to synthesize cDNA from total RNA. This kit utilizes oligo(dT)20 primer to target only mature mRNAs from total RNA content. Generation of cDNA was performed according to the manufacturer's protocol. The cDNA was stored at 4˚C. Real-time PCR was accomplished using Applied Biosystems™ TaqMan™ Universal Master Mix II, with uracil-N-glycosylase (UNG) and specific TaqMan™ gene expression primers listed in Supplemental Table 1 (Thermo Fisher, Invitrogen). The primers were designed to anneal to specific gene sequences encoding four different K_{ATP} channel subunits: Kir6.1, Kir6.2, SUR1, and SUR2. Additionally, GAPDH served as an amplification control.

Isolation of Lymphatic Muscle Cells

Freshly dissected mesenteric LVs were placed in a glass tube containing 500 µL of initial dissociation solution (Solution I) containing (in mmol/L): 145 NaCl, 4 KCl, 1 $MgCl_2$, 10 HEPES, 0.05 $CaCl_2$, 10 glucose, and 0.5 mg/mL bovine serum albumin; pH was adjusted to 7.4 using NaOH. After 10 minutes at room temperature, a glass bulb pipette was used to carefully remove Solution I and replace it with 500 µL of new dissociation solution (Solution II) containing 3.4 mg papain (1.7 mg/mL, Worthington 3119) and 2 mg of dithioerythritol stock (1 mg/mL, Sigma D8255). The LVs were incubated in this solution for 25 to 30 minutes at 37˚C before a glass bulb pipette was used to carefully remove solution II and replace it with 500 µL of enzyme solution (Solution III) containing 1 mg collagenase H (0.5 mg/mL, Sigma C8051), 1.4 mg collagenase F (0.7 mg/mL, Sigma C7926), and 2 mg trypsin

Downloaded from jpet.aspetjournals.org at ASPET Journals on April 18, 2024

JPET Fast Forward. Published on October 25, 2020 as DOI: 10.1124/jpet.120.000121
This article has not been copyedited and formatted. The final version may differ from this version.

inhibitor (1 mg/mL, Sigma T9128). After another 5 to 7 minutes at 37˚C, Solution III was similarly removed and the LVs were removed using a glass bulb pipette and placed in an Eppendorf tube containing 1 mL of the final enzyme solution (Solution IV), which contained 10 mg/mL collagenase I (Millipore Sigma SCR103), 1.5 mg/mL collagenase II (Worthington CLS-2), and 200 units/mL DNase (Alfa Aesar J62229). The Eppendorf tube was placed in an incubator (37^{o}C, 5% CO_2, Steri-Cycle CO_2 Incubator, Model 370, Marietta, OH, USA) and rotated using a MACSmix tube rotator (Miltenyi Biotec, Gladbach, Germany) for 30 minutes. Subsequently, the solution containing the dissociated LVs was spun at 0.5 g for 3 minutes to collect single LMCs. The cells were resuspended in 300 µL of isolation buffer (IB) composed of 0.5% bovine serum albumin and 2 mmol/L EDTA in phosphate-buffered saline, and spun down at 0.5 g for 3 minutes. This process was repeated twice more to wash the cells before they were directed to flow cytometry studies.

Flow Cytometry & ImageStream® Flow Cytometry

Once the rat mesenteric LMCs were isolated and washed, they were incubated with Kir6.1, Kir6.2, SUR1, or SUR2 primary antibodies (Supplemental Table 1) for 1 hour at room temperature in IB. These antibodies target subunit-specific protein sequences, a claim that we substantiated by searching epitope sequences of antibodies using BLAST (https://blast.ncbi.nlm.nih.gov). The specificities of anti-Kir6.1 and anti-Kir6.2 antibodies also have been validated in cells from Kir6.1$^{-/-}$ and Kir6.2$^{-/-}$ mice (Milovanova *et al*., 2005). Subsequently, the cells were washed and incubated with goat anti-rabbit IgG secondary antibody- Alexa 647 (1:500) and smooth muscle-specific α-actin-FITC (1:100) for 30 to 45 minutes. Then cells were washed three times with 1 mL of IB and resuspended in 300 µL IB for flow cytometry analysis. The data were collected using an Accari C6 flow cytometer (BD Biosciences, San Jose, CA, USA), and analyzed with FlowJo-V10 software (FlowJo LLC, Ashland, OR, USA) to provide information on the expression of distinct K_{ATP} channel subunit proteins in isolated LMCs.

To visually confirm that the antibody signal arose from single LMCs and not contaminating cell types, we also subjected isolated LMCs to imaging flow cytometry. The LMCs were incubated with primary antibodies (Supplemental Table 1) corresponding to Kir6.1 subunit (rabbit anti-rat, 1:50) and

Downloaded from jpet.aspetjournals.org at ASPET Journals on April 18, 2024

JPET Fast Forward. Published on October 25, 2020 as DOI: 10.1124/jpet.120.000121
This article has not been copyedited and formatted. The final version may differ from this version.

Kir6.2 subunit (guinea pig anti-rat, 1:50) for 1 to 1.5 hours at room temperature in IB. Subsequently, the LMCs were washed and incubated with two secondary antibodies, goat anti-rabbit IgG Cy3 (1:2000), goat anti-guinea pig Alexa 647 (1:2000), together with smooth muscle-specific α -actin-FITC (1:500) antibody, respectively, for 45 minutes. Then the cells were washed and resuspended in 50 µL of PBS. Finally, the suspensions of LMCs were imaged using an ImageStream®X Mk II Imaging Flow Cytometer (Luminex Corporation, Austin, TX, USA). Images were collected using IDEAS 6.2 software (Luminex Corporation, Austin, TX, USA).

Patch-Clamp Electrophysiology

Lymph vessels were subjected to enzymatic isolation as described for flow cytometry, except after incubation in 500 µL of Solution III, a drop of solution was visualized on an inverted microscope to ensure initial release of LMCs from LVs. The tube containing the LVs was then placed on ice, and a glass bulb pipette was used to remove Solution III and replace it with Solution I, free of enzymes. Gentle trituration resulted in the further separation of LMCs from residual LV tissue. The resulting suspension of LMCs was transported to a patch-clamp station, and aliquots of LMCs were transferred to a chamber mounted on the stage of an Olympus IMT-2 inverted microscope (Olympus Corporation, Shinjuki City, Tokyo, Japan) and allowed to settle before superfusion with high-K^+ bath solution of the following composition (in mmol/L): 145 KCl, 5 HEPES, 1.8 $CaCl_2$, and 1 $MgCl_2$, titrated to pH 7.4 with KOH. Patch pipettes were pulled from borosilicate glass (#7052, Garner Glass Co., Claremont, CA), fire-polished to a tip resistance of 5 to 8 MΩ, and filled with solution consisting of (in mmol/L): 145 KCl, 5 HEPES, 1.8 $CaCl_2$, and 1 $MgCl_2$, titrated to pH 7.4 with KOH. Slight suction was used to form a high resistance seal (>5 GΩ) between LMC membranes and the pipette tip to establish the cell-attached recording mode for recording of unitary K^+ currents. The patch potential was maintained at -50 mV for two minutes to record single-channel K^+ currents in drug-free bath solution. Subsequently, the chamber was filled with new bath solution containing 1 µmol/L cromakalim to activate K_{ATP} channels. Cromakalim-induced single-channel currents were recorded for 2 to 4 minutes at -50 mV, and then in

Downloaded from jpet.aspetjournals.org at ASPET Journals on April 18, 2024

JPET Fast Forward. Published on October 25, 2020 as DOI: 10.1124/jpet.120.000121
This article has not been copyedited and formatted. The final version may differ from this version.

10-mV steps using 2 minute increments at patch potentials between -70 mV to +50 mV. Current signals were amplified by an EPC-7 patch-clamp amplifier (List Medical Electronic, Darmstadt, Germany) connected to a TL-1 DMA Interface driven by pClamp 6.0 software (Axon Instruments, Foster City, CA) running an IBM-compatible computer for data acquisition and digitization. Analog to digital conversion was accomplished at a sampling rate of 5 kHz after signals were passed through an eight-pole Bessel filter with a cutoff frequency of 1 kHz to enable real-time visualization of small current amplitudes. After an average current-voltage relationship was generated by plotting unitary current amplitudes as a function of patch potential using Clampfit 10.3 software (Molecular Devices, San Jose, CA, USA) and GraphPad Prism 7 software (GraphPad Software, San Diego, CA, USA), the average unitary conductance of cromakalim-sensitive channels was calculated at negative patch potentials associated with linearity, and then again at positive patch potentials associated with inward rectification. In additional studies, the patch potential was maintained at -50 mV in drug-free bath solution for two minutes prior to filling the chamber with solution containing either 0.1 μmol/L minoxidil sulfate or 3 μmol/L diazoxide. Recordings at a patch potential of -50 mV were resumed to determine if these concentrations of KCOs, which caused half-inhibition of calculated flow in cannulated LVs, also activated a similar single-channel current as cromakalim in rat mesenteric LMCs.

Materials

Cromakalim, minoxidil sulfate and diazoxide were obtained from Sigma-Aldrich (St. Louis, MO, USA). Cromakalim and minoxidil sulfate were dissolved in dimethyl sulfoxide (DMSO) and stored as 50 mmol/L aliquots at -20ºC. Diazoxide was dissolved in 0.1 mol/L sodium hydroxide and stored as 50 mmol/L aliquots at -20ºC. Phenylephrine was dissolved in pure water as 10 mmol/L aliquots and stored at -20ºC.

Statistics

Data obtained from control and treated groups were expressed as mean ± standard deviation, and compared using the unpaired t-test or one-way ANOVA, as applicable. All differences were judged to

Downloaded from jpet.aspetjournals.org at ASPET Journals on April 18, 2024

JPET Fast Forward. Published on October 25, 2020 as DOI: 10.1124/jpet.120.000121
This article has not been copyedited and formatted. The final version may differ from this version.

be significant at the level of $P < 0.05$. Sample sizes were determined assuming standard deviations equal to 20% of the mean of the control group and a 30% change of the mean in experimental groups with power = 0.8-0.9, $\alpha = 0.05$ and $\beta = 0.20$. Flow cytometry data were repeated in triplicate.

Results

KCOs inhibit the rhythmic contractions of isolated LVs

Increasing concentrations of the prototypic KCO, cromakalim, inhibited and ultimately abolished the rhythmic contractions of rat mesenteric LVs (Fig. 1). Addition of the corresponding DMSO solvent did not significantly affect contraction parameters (Fig. 1 & Suppl. Table 2). Cromakalim significantly impaired flow through LVs at concentrations higher than 0.18 µmol/L by attenuating the frequency and amplitude of rhythmic contractions (Fig. 3 & Table 1). Consistent with the hyperpolarizing effect of KCOs on LMCs that drives the resting membrane potential further from the threshold for action potential firing (Mathias and von der Weid, 2013), contraction frequency was most sensitive to concentration-dependent inhibition by KCOs. In contrast, contraction amplitude failed to show progressive inhibition by increasing concentrations of KCOs. Instead contractions abruptly ceased at a given KCO concentration, which varied slightly between different LVs. This all-or-none response is reflected in the steep negative relationship between KCO concentration and amplitude in Figure 3, and accounts for the high standard deviation values. Cromakalim also increased EDD, an effect predicted to promote flow by increasing filling volume between contractions, and thereby stroke volume, but the effect on EDD was mild (≤5%) compared to the profound negative effect of cromakalim on contraction frequency and amplitude. Notably, we implicated K_{ATP} channels in cromakalim-induced inhibition of rhythmic contractions by demonstrating that 1 µmol/L glibenclamide, a K_{ATP} channel antagonist, caused a rightward shift in the IC_{50} of cromakalim for contraction frequency and amplitude (Suppl Fig. 1). We avoided using higher concentrations of glibenclamide, which are known to lose selectivity for K_{ATP} channels (Bessadok *et al.*, 2011; Simard *et al.*, 2012).

Downloaded from jpet.aspetjournals.org at ASPET Journals on April 18, 2024

JPET Fast Forward. Published on October 25, 2020 as DOI: 10.1124/jpet.120.000121
This article has not been copyedited and formatted. The final version may differ from this version.

Next, we explored the effect of clinically available KCOs on the contractile activity of isolated LVs. Increasing half-log (0.01-100 µmol/L) concentrations of either minoxidil sulfate or diazoxide inhibited the rhythmic contractions of isolated LVs (Fig. 2), but with markedly different potencies. The potency of minoxidil sulfate was comparable to cromakalim (Fig. 3); minoxidil sulfate exhibited IC_{50} values of 0.35 µmol/L and 1.82 µmol/L for contraction frequency and amplitude, respectively, compared to cromakalim's IC_{50} values of 0.25 µmol/L and 0.77 µmol/L for the same parameters. Intraluminal flow was attenuated significantly by 0.1 µmol/L minoxidil sulfate and its IC_{50} value of 0.47 µmol/L is within the clinically achievable peak plasma concentration of 0.48 µmol/L observed in chronic hypertensive patients administered minoxidil (Lowenthal and Affrime, 1980). This IC_{50} value also is well within the range of 0.2 µmol/L to 1.2 µmol/L reported for therapeutic plasma concentrations (TIAFT, 2004).

Diazoxide inhibited rhythmic contractions in rat mesenteric lymph vessels at much higher concentrations compared to cromakalim and minoxidil sulfate (Figs. 2 & 3; Table 1). The inhibition of contraction amplitude by diazoxide was very abrupt, exhibiting an IC_{50} value of 30.2 µmol/L, which represented a 16.56–fold higher value compared to minoxidil sulfate. Similarly, the IC_{50} value of 8.3 µmol/L for diazoxide inhibition of contraction frequency was 233.8-fold higher compared to minoxidil sulfate. Diazoxide only inhibited intraluminal flow at concentrations ≥ 3 µmol/L. However, the therapeutic plasma concentrations of diazoxide reportedly range between 145 to 332 µmol/L (Neary *et al.*, 1973). Thus, the entire concentration range of diazoxide tested in the present study was easily within clinically achievable plasma concentrations.

KCOs decrease mesenteric lymph flow *in vivo*

Our finding that clinical KCOs inhibit intraluminal flow through isolated lymph vessels at therapeutic plasma concentrations pointed to the importance of determining whether this effect translates to lymph flow *in vivo*. For these studies, we focused on minoxidil sulfate as the clinical KCO with the highest potency for disrupting rhythmic contractions in isolated LVs. Similar to our in vitro studies, we utilized cromakalim in parallel studies as this prototypic KCO is regarded as the most selective activator of K_{ATP}

Downloaded from jpet.aspetjournals.org at ASPET Journals on April 18, 2024

JPET Fast Forward. Published on October 25, 2020 as DOI: 10.1124/jpet.120.000121
This article has not been copyedited and formatted. The final version may differ from this version.

channels. Superfusion of the mesenteric lymphatic circulation with increasing log concentrations (0.01-10 μmol/L) of cromakalim abruptly inhibited positive volumetric lymph flow *in vivo* at concentrations ≥ 0.1 μmol/L (Fig. 4 & Table 2). Minoxidil sulfate also exhibited a concentration-dependent inhibition of positive volumetric lymph flow in vivo, exhibiting significant slowing of flow at 1 μmol/L (Fig. 4 and Table 2), a concentration corresponding to patient plasma concentrations (Lowenthal and Affrime, 1980; TIAFT, 2004; Zarghi *et al.*, 2004). Superfusion of a similar solvent concentration of corresponding DMSO did not significantly alter lymph flow.

Rat mesenteric LMCs primarily express Kir6.1, Kir6.2 and SUR2

Next, we considered whether LMCs might express a unique population of K_{ATP} channels considering that they represent “hybrid” cells with properties of smooth and striated muscle. In this series of studies, we initially defined subunit transcripts in rat mesenteric LVs using RT-PCR (Table 3). These results indicated the presence of both Kir6.1 and Kir6.2 transcripts. Expression level of the SUR2 transcript was comparable to Kir6.1, whereas the SUR1 transcript only was detected at a high cycle threshold suggesting low expression. The small quantity of RNA obtained from LVs limited our analysis to using validated TaqMan^{TM} primers to differentiate K_{ATP} channel subunits. We did not differentiate between the SUR2A/B splice variants that lack validated TaqMan^{TM} primers. GAPDH was used as a quality control amplicon to ensure consistent amplification between different vessel samples (n=3). However, the cDNA for these studies was obtained from whole lymph vessels, which contain multiple cell types that potentially express variable types of K_{ATP} channels. Thus, further studies were performed to define the protein expression of K_{ATP} channel subunits in purified populations of LMCs. Isolated LMCs were co-stained with the smooth muscle marker, α-SMA-FITC, and antibodies directed against either the Kir6.1, Kir6.2, SUR1 or SUR2 subunit. LMCs were incubated subsequently with the secondary antibody conjugated to Alexa-Fluor 647, and then subjected to flow cytometry. The α-SMA-FITC stain was used to set the gate that defined the LMC population (Fig. 5A). Next, we used a negative control, which consisted of LMCs incubated with α-SMA-FITC and the Alexa-Fluor 647 conjugated secondary antibody without primary antibodies to control for any non-specific positive

Downloaded from jpet.aspetjournals.org at ASPET Journals on April 18, 2024

JPET Fast Forward. Published on October 25, 2020 as DOI: 10.1124/jpet.120.000121
This article has not been copyedited and formatted. The final version may differ from this version.

staining of the secondary antibody within the gated region (Fig. 5B). Using these gates, we then measured the Alexa-Fluor 647 signals in the LMC samples incubated with primary antibodies as described above. Flow cytometry detected immunoreactivity corresponding to protein expression of Kir6.1, Kir6.2, and SUR2. In contrast, SUR1 immunoreactivity was not detected on the cell surface (Fig. 5C-E), supporting data from our gene expression studies that indicated rare SUR1 transcripts (Table 3). In the α-SMA positive gated cells (Fig. 5B), we found that 37.09% of the cells stained positive for Kir6.1 expression (Fig. 5C), 11.75% stained positive for Kir6.2 expression (Fig. 5D), and 33.14% stained positive for in SUR2 expression (Fig. 5F). We did not observe any positive SUR1 staining in the gated region (Fig. 5E). Flow cytometry with ImageStream® visually confirmed the fluorescent signals were localized to single LMCs rather than representing artifact or signals from other cell types not fully dissociated from LMCs (Fig. 6). Interestingly, ImageStream® results (Fig. 6) also indicated that the Kir6.1 and Kir6.2 subunits are co-expressed on the same LMCs.

In follow-up studies, we applied the patch-clamp technique to provide initial information on whether Kir6.1 and/or Kir6.2 subunits co-assemble to form the tetrameric structure of functional K_{ATP} channels in rat mesenteric LMCs. Earlier studies suggest that homotetrameric K_{ATP} channels composed of Kir6.1 and SUR2B subunits exhibit a single-channel conductance of 29.4 pS, whereas homotetrameric Kir6.2 pore structures exhibit a higher single-channel conductance of 60.2 pS in symmetrical K^+ recording solutions. Corresponding Kir6.1/6.2 heterotetramers show a hybrid conductance of approximately 47.5 ± 1.6 pS (Cui *et al.*, 2001). Using patch pipettes filled with 145 mmol/L KCl applied to cell-attached patches of LMCs, single-channel currents were rarely detected at a patch potential of -50 mV in drug-free bath solution (Fig. 7A). The negative patch potential of -50 mV was chosen to silence voltage-gated K^+ channels, which presumably are expressed in LMCs similar to other types of muscle cells. However, within 5 minutes exposure to 1 μmol/L cromakalim in the bath solution, single-channel currents were detected in the majority (16/19) of patches (Fig. 7B) and cromakalim activation was progressive, revealing multiple channels evident as stacked current openings in some patches (not

Downloaded from jpet.aspetjournals.org at ASPET Journals on April 18, 2024

JPET Fast Forward. Published on October 25, 2020 as DOI: 10.1124/jpet.120.000121
This article has not been copyedited and formatted. The final version may differ from this version.

shown). In most patches, channel open-state probability continued to increase for the duration of experiments, which generally ended because of loss of the high resistance seal between 10 and 20 minutes after exposure to drug. This confounding factor prevented us from performing studies to reverse cromakalim-elicited channel activation using K_{ATP} channel-specific antagonists. Alternatively, we focused on defining the single-channel conductance of cromakalim-elicited K^+ current and the response of cell-attached patches of LMCs to additional KCOs.

Accordingly, cromakalim-induced unitary currents were recorded in 2-minute intervals at patch potentials (10-mV steps) between -70 mV and +50 mV, and current amplitude was plotted as a function of patch potential to obtain a current-voltage relationship (Fig. 7C). Because K_{ATP} channels show weak inward rectification (i.e., conduct current more readily at negative compared to positive patch potentials), we focused our recordings at negative patch potentials in order to calculate single-channel conductance between -70 mV and -30 mV. A single-channel conductance of 46.4 pS was resolved, indicative of heterotetrameric K_{ATP} channels composed of Kir6.1/6.2 subunits. The lower single-channel conductance of 33.6 pS at positive patch potentials confirmed the presence of weak inward rectification (Fig. 7C), which is a property of K_{ATP} channels including Kir6.1/6.2 heterotetrameric channels that only weakly rectify (Cui *et al.*, 2001; Acevedo *et al.*, 2006; Wu *et al*., 2007). We presume these apparent functional Kir6.1/6.2 pore-forming structures co-assemble with the abundant SUR2 subunits detected by flow cytometry to form functional K_{ATP} channels in LMCs.

In a final series of cell-attached patch-clamp studies, LMCs were exposed to 0.1 μmol/L minoxidil sulfate and 3 μmol/L diazoxide to determine whether these concentrations of KCOs, which reduced calculated flow in isolated LVs by ~50% (Figure 3D), elicited unitary currents of similar amplitude as cromakalim in the corresponding LMCs, implying targeting of the same K_{ATP} channel. Notably, these concentrations of minoxidil sulfate and diazoxide are within the range of clinical plasma concentrations. Similar to our earlier patch-clamp studies in which 1 μmol/L cromakalim elicited an inward current with an amplitude of 2.67 ± 0.12 pA at a patch potential of -50 mV (Figure 7), 0.1 μmol/L minoxidil sulfate

Downloaded from jpet.aspetjournals.org at ASPET Journals on April 18, 2024

JPET Fast Forward. Published on October 25, 2020 as DOI: 10.1124/jpet.120.000121
This article has not been copyedited and formatted. The final version may differ from this version.

and 3 μmol/L diazoxide also elicited inward currents at a patch potential of -50 mV with average unitary amplitudes of 2.51 ± 0.07 pA and 2.58 ± 0.13 pA, respectively (n = 4 patches each) under the same condition (Figure 8C-F). In parallel control studies using the DMSO solvent, no unitary currents were observed during recording periods as long as 20 to 30 minutes (Figure 8A-B). Thus, all three KCOs included in this study shared activation of a channel of similar current amplitude. Interestingly, in a single patch not included in the analysis, minoxidil sulfate elicited a clearly lower amplitude current (1.6 pA), corresponding to a presumed single-channel conductance of 32 pS. Although only an isolated observation, this finding was consistent with the single-channel conductance of 29.4 pS associated with Kir6.1 homotetrameric K_{ATP} channels. Collectively, our patch-clamp findings were consistent with the expression of a preponderance of Kir6.1/6.2 channels in rat mesenteric LMCs with potential inclusion of K_{ATP} channels of other pore-forming subunit compositions.

Discussion

The present study provides three new findings that may shed light on the mechanisms by which clinical KCOs cause peripheral edema as an off-target effect. First, minoxidil sulfate and diazoxide, in concentrations achieved in plasma samples of patients, progressively attenuate and ultimately interrupt the rhythmic contractions of isolated LVs. Inhibition of contraction frequency appears to be the key effect by which KCOs disrupt rhythmic contractions and mitigate intraluminal flow under these conditions. Second, minoxidil sulfate also compromises lymph flow in vivo at clinically relevant concentrations. Third, immune-imaging of K_{ATP} channel proteins combined with patch-clamp analysis of cromakalim-elicited K^+ currents suggests that functional K_{ATP} channels in LMCs represent Kir6.1/6.2 heterotetramers co-assembled with SUR2 subunits. In contrast, the predominant K_{ATP} channels in arterial SMCs are presumed to be Kir6.1 homotetrameric channels (Mannhold, 2004; Jahangir and Terzic, 2005; Rubaiy, 2016). Thus, the population of K_{ATP} channels expressed by LMCs may differ from arterial SMCs, inferring an opportunity to design new KCOs that only target arterial K_{ATP} channels to avoid disrupting lymphatic contractions and lymph flow.

Downloaded from jpet.aspetjournals.org at ASPET Journals on April 18, 2024

JPET Fast Forward. Published on October 25, 2020 as DOI: 10.1124/jpet.120.000121
This article has not been copyedited and formatted. The final version may differ from this version.

The primary emphasis of our study was to determine whether the clinical KCOs, minoxidil sulfate and diazoxide, disrupt lymphatic contractions and lymph flow at concentrations measured in samples of human plasma. However, we also used cromakalim in our study because it has been characterized extensively as a prototypic, first generation K_{ATP} channel –selective agonist (Mannhold, 2004). Earlier studies reported that cromakalim hyperpolarized guinea pig and rat mesenteric LMCs, thereby inhibiting the voltage-dependent Ca^{2+} influx that mediates the rhythmic contractions of collecting LVs (Von der Weid, 1998; Gashev, 2002; Imtiaz *et al.*, 2007; Dougherty *et al.*, 2008; Davis *et al.*, 2011, 2012; Mathias and von der Weid, 2013; Scallan et al., 2013). Additionally, the use of cromakalim helped ensure congruence between our lymphatic preparation and those of earlier studies. In this regard, our calculated IC_{50} value of 0.247 µmol/L for cromakalim-induced inhibition of contractile frequency in rat mesenteric lymph vessels closely resembles the IC_{50} value of 0.126 µmol/L reported in guinea pig mesenteric lymph vessels (Mathias and von der Weid, 2013).

Importantly, the subunit composition of K_{ATP} channels primarily determines their biophysical and pharmacological properties including sensitivity to KCOs. Therefore, we employed a combination of functional and molecular techniques to explore the composition of K_{ATP} channels in the lymphatic vasculature. In this regard, four Kir6.1 and/or Kir6.2 subunits co-assemble as homo- or hetero-tetramers to form the K_{ATP} channel pore, which confers the properties of K^+-selectivity and single-channel conductance. Accessory sulfonylurea receptor subunits (SUR1 or SUR2A/B) co- assemble in a ratio of 4:4 with the Kir6.x subunits to form the fully functional K_{ATP} channel (Foster and Coetzee, 2016). Structurally different KCO families bind preferentially to either SUR1 or SUR2 subunits to regulate cell excitability in a tissue-specific manner (Mannhold, 2004; Jahangir and Terzic, 2005; Foster and Coetzee, 2015). Cromakalim, the prototypic KCO, binds to SUR2A and SUR2B (Matsuo *et al.*, 2000; Tricarico *et al.*, 2008; Nichols *et al.*, 2013). In contrast, the preferential binding of minoxidil sulfate, the active metabolite of minoxidil, to SUR2B explains its potent vasodilator and antihypertensive effect, because arterial SMCs primarily express Kir6.1/SUR2B complexes (Gopalakrishnan *et al.*, 1993). The

Downloaded from jpet.aspetjournals.org at ASPET Journals on April 18, 2024

JPET Fast Forward. Published on October 25, 2020 as DOI: 10.1124/jpet.120.000121
This article has not been copyedited and formatted. The final version may differ from this version.

different pharmacological profiles of cromakalim and minoxidil sulfate also may relate to different binding sites on the SUR2 subunit for the two KCOs, which is suggested by the fact that glibenclamide noncompetitively antagonizes minoxidil sulfate, but competitively antagonizes cromakalim (Wickenden *et al.*, 1991). Finally, diazoxide has been described as a weakly acting KCO (Mannhold, 2004), but it exhibits equal affinity for SUR1 and SUR2B but not SUR2A (Matsuo *et al.*, 2000; Matsuoka *et al.*, 2000). Accordingly, it avidly binds to Kir6.2/SUR1 channels expressed by pancreatic β cells to enact membrane hyperpolarization and inhibition of Ca^{2+}-dependent insulin release, thereby providing a valuable therapeutic for the treatment of persistent hyperinsulinism. Its dual affinity for vascular Kir6.1/SUR2B channels also explains its continued use for the treatment of malignant hypertension (Jahangir and Terzic, 2005).

Notably, clinically achievable plasma concentrations of minoxidil sulfate range between 0.2 µmol/L and 1.2 µmol/L (TIAFT, 2004), whereas therapeutic plasma concentrations of diazoxide are many-fold higher and range between 43.3 µmol/L and 216.7 µmol/L (TIAFT, 2004). Both KCO medications can cause severe peripheral edema (Mehta *et al.*, 1975; Pettinger and Mitchell, 1988; Herrera *et al.*, 2018). For our ex vivo studies in isolated LVs, the resulting IC_{50} values for minoxidil sulfate and diazoxide - induced inhibition of intraluminal flow were well within clinically achievable plasma concentrations. We further explored whether KCOs disrupted lymph flow in vivo. Again, using cromakalim as the KCO prototype, we initially superfused mesenteric loops with progressive concentrations of cromakalim in order to control the concentration of drug delivered to the lymphatic vasculature. Our *in vivo* results demonstrate that cromakalim also markedly compromises flow in the intact lymphatic circulation. Additional studies revealed that minoxidil sulfate also reduced lymph flow at concentrations beginning at 1 µmol/L, which is within the range of clinically achievable plasma concentrations for this antihypertensive medication (TIAFT, 2004). To our knowledge, the latter finding provides the first direct evidence that KCOs can severely compromise lymph flow in vivo. Interestingly, patients with Cantú syndrome, which is a disease caused by gain-of-function mutations of K_{ATP} channels, also exhibit

Downloaded from jpet.aspetjournals.org at ASPET Journals on April 18, 2024

JPET Fast Forward. Published on October 25, 2020 as DOI: 10.1124/jpet.120.000121
This article has not been copyedited and formatted. The final version may differ from this version.

edema similar to patients administered KCOs for extended periods of time (Mehta *et al.*, 1975; Sica, 2004; Harakalova *et al.*, 2012; Nichols *et al.*, 2013; Scallan *et al.*, 2013).

A single earlier report indicated that whole LVs from the guinea pig mesentery primarily express Kir6.1 and SUR2B transcripts, similar to vascular SMCs (Newgreen *et al.*, 1990; Mathias and von der Weid, 2013). Here, we utilized a multi-faceted approach to conclude that functional K_{ATP} channels in LMCs primarily represent Kir6.1/6.2 complexes co-assembled with SUR2. In this regard, pharmacological studies revealed that both cromakalim and minoxidil sulfate mitigate lymphatic contractions, but they show low affinity for the SUR1 subunit, implicating SUR2 as their binding site in LMCs (Davies *et al.*, 2005; Zarzoso *et al.*, 2018). Second, our gene amplification studies using RNA extracted from whole LVs revealed Kir6.1 and Kir6.2 transcripts in similar abundance, and SUR2 transcript in overwhelming preponderance to SUR1. Third, immune-imaging of purified populations of cell-sorted LMCs confirmed the co-expression of Kir6.1, Kir6.2, and SUR2 proteins on the surface of single LMCs, but failed to detect SUR1. Finally, our patch-clamp studies revealed a slope conductance more consistent with hybrid heterodimerized Kir6.1/6.2 channels than homotetrameric Kir6.1 or 6.2 channels (Cui *et al.*, 2001). Only a single patch revealed a minoxidil-elicited lower-amplitude current more consistent with a Kir6.1 homotetramer structure. Thus, although some structural homogeneity is possible, our collective findings suggest that K_{ATP} channels in rat mesenteric LMCs represent Kir6.1/Kir6.2 pore structures co-assembled with regulatory SUR2 subunits, In this respect, K_{ATP} channels in LMCs may be molecularly unique from their counterparts in the arterial vasculature, which appear to be predominantly Kir6.1 homo-tetramers co-assembled with SUR2.

The present study has several limitations. First, we used the rat mesenteric lymphatic circulation in our study because it is amenable to high-speed optical imaging. However, further studies are needed to ensure our findings translate to other lymphatic circulations including those of humans. Second, it's possible that the concentrations of KCOs may differ between plasma, interstitial fluid and lymph after systemic administration. In our study, we assumed that LVs would be exposed to plasma

Downloaded from jpet.aspetjournals.org at ASPET Journals on April 18, 2024

JPET Fast Forward. Published on October 25, 2020 as DOI: 10.1124/jpet.120.000121
This article has not been copyedited and formatted. The final version may differ from this version.

concentrations of KCOs in vivo after systemic administration of these medications, but we failed to find information to help us predict the pattern of KCO partitioning. Finally, instead of infusing the KCOs systemically, we chose to topically apply cromakalim and minoxidil sulfate to determine the effect of KCOs on mesenteric lymph flow in vivo. Topical application ensured tight control of KCO concentration at the level of the LV and guaranteed an absence of KCO-elicited systemic effects that could have confounded interpretation of results. In contrast, systemic administration is potentially fraught with difficulties in data interpretation due to the poorly characterized pharmacokinetic profiles of minoxidil sulfate and diazoxide in rats and the unintended effects of KCOs on blood pressure that could indirectly affect capillary filtration and thereby lymph flow.

In summary, it is assumed that KCOs cause edema by strongly dilating arterioles and increasing capillary pressure to promote fluid movement from the intravascular to the interstitial space (Sica, 2003; Mortimer and Levick, 2004). However, our findings suggest that KCO medications at clinically relevant plasma concentrations also directly disrupt lymphatic contractions and lymph flow as another potential mechanism of edema formation. Finally, our new evidence that K_{ATP} channels in rat mesenteric LMCs may predominantly represent Kir6.1/6.2 heterotetramers co-assembled with SUR2, implies that LMCs may express K_{ATP} channel populations that differ from the predominantly Kir6.1 homotetrameric channels of the arterial circulation. In this regard, the KCOs in clinical practice are known to bind to sulphonylurea receptors to disinhibit arterial Kir6.1 channels and induce vasodilation. However, it is conceivable that the co-assembly of Kir6.1 and Kir6.2 subunits in LMCs may provide a novel 3-D structure containing binding domains with lower affinity for novel pore-targeting KCOs than their arterial counterparts. In this case, it may be possible to design new KCOs that bind selectively to K_{ATP} channels in arterial SMCs to mediate vasodilation, but avoid activation of the K_{ATP} channels in LMCs to prevent peripheral edema or ameliorate its severity.

Authorship Contributions:

Participated in research design: Garner, Rusch, Mu

Downloaded from jpet.aspetjournals.org at ASPET Journals on April 18, 2024

JPET Fast Forward. Published on October 25, 2020 as DOI: 10.1124/jpet.120.000121
This article has not been copyedited and formatted. The final version may differ from this version.

Conducted experiments: Garner, Stolarz, Stuckey, Liu

Contributed new reagents or analytical tools: Sarimolloaglu

Performed data analysis: Garner, Stolarz, Rusch, Mu

Wrote or contributed to the writing of the manuscript: Garner, Stolarz, Palade, Rusch, Mu

References:

Acevedo JJ, Mendoza-Lujambio I, de la Vega-Beltran JL, Trevino CL, Felix R, Darszon A. K_{ATP} channels in mouse spermatogenic cells and sperm, and their role in capacitation. (2006) *Developmental Biol* **289**:395-405.

Akopova OV (2017) Direct and off-target effects of ATP-sensitive potassium channels opener diazoxide. *J Drug Metab Toxicol* **8**:1-8.

Bessadok A, Garcia E, Jacquet H, Martin S, Garrigues A, Loiseau N, André F, Orlowski S, and Vivaudou M (2011) Recognition of sulfonylurea receptor (ABCC8/9) ligands by the multidrug resistance transporter P-glycoprotein (ABCB1): functional similarities based on common structural features between two multispecific ABC proteins. *J Biol Chem* **286**:3552–3569.

Bryan J (2011) How minoxidil was transformed from an antihypertensive to hair-loss drug. *Pharm J* **287**:137.

Choi I, Lee S, and Hong Y (2012) The new era of the lymphatic system : no longer secondary to the blood vascular system. *Cold Spring Harb Perspect Med* **2**:1-23.

Coetzee WA (2013) Multiplicity of effectors of the cardioprotective agent, diazoxide. *Pharmacol Ther* **140**:167-175.

Cui Y, Giblin JP, Clapp LH, and Tinker A (2001) A mechanism for ATP-sensitive potassium channel diversity: functional coassembly of two pore-forming subunits. *Proc Natl Acad Sci U S A* **98**:729–734.

Downloaded from jpet.aspetjournals.org at ASPET Journals on April 18, 2024

JPET Fast Forward. Published on October 25, 2020 as DOI: 10.1124/jpet.120.000121
This article has not been copyedited and formatted. The final version may differ from this version.

Davies GC, Thornton MJ, Jenner TJ, Chen YJ, Hansen JB, Carr RD, and Randall VA (2005) Novel and established potassium channel openers stimulate hair growth in vitro: implications for their modes of action in hair follicles. *J Invest Dermatol* **124**:686–694.

Davis MJ, Rahbar E, Gashev AA, Zawieja DC, and Moore JE (2011) Determinants of valve gating in collecting lymphatic vessels from rat mesentery. *Am J Physiol Circ Physiol* **301**:H48–H60.

Davis MJ, Scallan JP, Wolpers JH, Muthuchamy M, Gashev AA, and Zawieja DC (2012) Intrinsic increase in lymphangion muscle contractility in response to elevated afterload. *Am J Physiol Circ Physiol* **303**:H795–H808.

Dörschner H, Brekardin E, Uhde I, Schwanstecher C, and Schwanstecher M (1999) Stoichiometry of sulfonylurea-induced ATP-sensitive potassium channel closure. *Mol Pharmacol* **55**:1060–1066.

Dougherty PJ, Davis MJ, Zawieja DC, and Muthuchamy M (2013) Calcium sensitivity and cooperativity of permeabilized rat mesenteric lymphatics. *Am J Physiol Integr Comp Physiol* **294**:R1524–R1532.

Foster MN, and Coetzee WA (2016) K_{ATP} channels in the cardiovascular system. *Physiol Rev* **96**:177–252.

Gashev AA (2002) Physiologic aspects of lymphatic contractile function: current perspectives. *Ann N Y Acad Sci* **979**:178–187.

Gopalakrishnan M, Janis RA, and Triggle DJ (1993) ATP-sensitive K^+ channels: pharmacologic properties, regulation, and therapeutic potential. *Drug Dev Res* **28**:95–127.

Harakalova M, van Harssel JJT, Terhal PA, van Lieshout S, Duran K, Renkens I, Amor DJ, Wilson LC, Kirk EP, Turner CLS, Shears D, Garcia-Minaur S, Lees MM, Ross A, Venselaar H, Vriend G, Takanari H, Rook MB, van der Heyden MAG, Asselbergs FW, Breur HM, Swinkels ME, Scurr IJ, Smithson SF, Knoers N V, van der Smagt JJ, Nijman IJ, Kloosterman WP, van Haelst MM, van Haaften G, and

Downloaded from jpet.aspetjournals.org at ASPET Journals on April 18, 2024

JPET Fast Forward. Published on October 25, 2020 as DOI: 10.1124/jpet.120.000121
This article has not been copyedited and formatted. The final version may differ from this version.

Cuppen E (2012) Dominant missense mutations in ABCC9 cause Cantú syndrome. *Nat Genet* **44**:793–796.

Herrera A, Ellen Vajravelu M, Givler S, Mitteer L, Avitabile CM, Lord K, and De León DD (2018) Prevalence of adverse events in children with congenital hyperinsulinism treated with diazoxide. *J Clin Endocrinol Metab* **103**:4235–4372.

Imtiaz MS, Zhao J, Hosaka K, von der Weid PY, Crowe M, and van Helden DF (2007) Pacemaking through Ca^{2+} stores interacting as coupled oscillators via membrane depolarization. *Biophys J* **92**:3843–3861.

Jahangir A and Terzic A (2005) K_{ATP} channel therapeutics at the bedside. *J Mol Cell Cardiol* **39**:99–112.

Lexicomp (2020) Diazoxide (Lexi-Drugs) https://online.lexi.com/lco/action/doc/retrieve/docid/patch_f/6729?cesid=2JtH6XyTRqQ&searchUrl=%2Flco%2Faction%2Fsearch%3Fq%3Ddiazoxide%26t%3Dname%26va%3Ddiazoxide.

Lowenthal DT and Affrime MB (1980) Pharmacology and pharmacokinetics of minoxidil. *J Cardiovasc Pharmacol* **2**:S93–S106.

Mannhold R (2004) K_{ATP} openers: structure-activity relationships and therapeutic potential. *Med Res Rev* **24**:213–266.

Mathias R, and von der Weid PY (2013) Involvement of the NO-cGMP-K_{ATP} channel pathway in the mesenteric lymphatic pump dysfunction observed in the guinea pig model of TNBS-induced ileitis. *Am J Physiol Gastrointest Liver Physiol* **304**:G623–G634.

Matsuo M, Tanabe K, Kioka N, Amachi T, and Ueda K (2000) Different binding properties and affinities for ATP and ADP among sulfonylurea receptor subtypes, SUR1, SUR2A, and SUR2B. *J Biol Chem* **275**:28757-28763.

Downloaded from jpet.aspetjournals.org at ASPET Journals on April 18, 2024

JPET Fast Forward. Published on October 25, 2020 as DOI: 10.1124/jpet.120.000121
This article has not been copyedited and formatted. The final version may differ from this version.

Matsuoka T, Matsushita K, Katayama Y, Fujita A, Inageda K, Tanemoto M, Inanobe A, Yamashita S, Matsuzawa Y, and Kurachi Y (2000) C-terminal tails of sulfonylurea receptors control ADP-induced activation and diazoxide modulation of ATP-sensitive K^+ channels. *Circ Res* **87**:873–880.

Mehta PK, Mamdani B, Shansky RM, Mahurkar SD, and Dunea G (1975) Severe hypertension. *JAMA* **233**:249-252.

Milovanova T, Chatterjee S, Manevich Y, Kotelnikova I, DeBolt K, Madesh M, Moore JS, and Fisher AB (2005) Lung endothelial cell proliferation with decreased shear stress is mediated by reactive oxygen species. *Am J Physiol Cell Pysiol.* **290**:C66-C76.

Mortimer PS, and Levick JR (2004) Chronic peripheral oedema: the critical role of the lymphatic system. *Clin Med* **4**:448–453.

Mortimer PS and Rockson SG (2014) New developments in clinical aspects of lymphatic disease. *J Clin Invest* **124**:915-921.

Muthuchamy M, Gashev A, Boswell N, Dawson N, and Zawieja D (2003) Molecular and functional analyses of the contractile apparatus in lymphatic muscle. *FASEB J* **17**:920–922.

Neary D, Thurston H, and Pohl JEF (1973.) Development of extrapyramidal symptoms in hypertensive patients treated with diazoxide. *B Med J* **3**:474-475.

Newgreen DT, Bray KM, McHarg AD, Weston AH, Duty S, Brown BS, Kay PB, Edwards G, Longmore J, and Southerton JS (1990) The action of diazoxide and minoxidil sulphate on rat blood vessels: a comparison with cromakalim. *Br J Pharmacol* **100**:605–613.

Nichols CG, Singh GK, and Grange DK (2013) K_{ATP} channels and cardiovascular disease: suddenly a syndrome. *Circ Res* **112**:1059–1072.

Nipper ME and Dixon JB (2013) Engineering the lymphatic system. *Cardiovasc Eng Technol* **2**:296–308.

Downloaded from jpet.aspetjournals.org at ASPET Journals on April 18, 2024

JPET Fast Forward. Published on October 25, 2020 as DOI: 10.1124/jpet.120.000121
This article has not been copyedited and formatted. The final version may differ from this version.

Noma A (1983) ATP-regulated K^+ channels in cardiac muscle. *Nature* **305**:147–148.

Pettinger WA and Mitchell HC (1988) Side effects of vasodilator herapy. *Hypertension* **11**:34-36.

Rubaiy HN (2016) The therapeutic agents that target ATP-sensitive potassium channels. *Acta Pharm* **66**:23–34.

Sarimollaoglu M, Stolarz AJ, Nedosekin DA, Garner BR, Fletcher TW, Galanzha EI, Rusch NJ, and Zharov VP (2018) High-speed microscopy for in vivo monitoring of lymph dynamics. *J Biophotonics* e201700126.

Scallan JP, Wolpers JH, and Davis MJ (2013) Constriction of isolated collecting lymphatic vessels in response to acute increases in downstream pressure. *J Physiol* **591**:443–459.

Shi WW, Yang Y, Shi Y, and Jiang C (2012) K(ATP) channel action in vascular tone regulation: from genetics to diseases. *Sheng Li Xue Bao* **64**:1–13.

Sica DA (2003) Calcium channel blocker-related peripheral edema: can it be resolved? *J Clin Hypertens* **5**:291–295.

Sica DA (2004) Minoxidil: An underused vasodilator for resistant or severe hypertension. *J Clin Hypertens* **6**:283–287.

Simard JM, Tsymbalyuk O, Keledjian K, Ivanov A, Ivanova S, and Gerzanich V (2012) Comparative effects of glibenclamide and riluzole in a rat model of severe cervical spinal cord injury. *Exp Neurol* **233**:566–574.

Stolarz AJ, Sarimollaoglu M, Marecki JC, Fletcher TW, Galanzha EI, Rhee SW, Zharov VP, Klimberg VS, and Rusch NJ (2019) Doxorubicin activates ryanodine receptors in rat lymphatic muscle cells to attenuate rhythmic contractions and lymph flow. *J Pharmacol Exp Ther* **371**:278–289.

Downloaded from jpet.aspetjournals.org at ASPET Journals on April 18, 2024

JPET Fast Forward. Published on October 25, 2020 as DOI: 10.1124/jpet.120.000121
This article has not been copyedited and formatted. The final version may differ from this version.

Telinius N, Kim S, Pilegaard H, Pahle E, Nielsen J, Hjortdal V, Aalkjaer C, and Boedtkjer DB (2014) The contribution of K^+ channels to human thoracic duct contractility. *Am J Physiol Heart Circ Physiol* **307**:H33-H43.

TIAFT (2004) Uges DRA: TIAFT reference blood level list of therapeutic and toxic substances. *Int Assoc Forensic Toxicol* Accessed 05.20.2020.

Tricarico D, Mele A, Liss B, Ashcroft FM, Lundquist AL, Desai RR, George AL, and Conte CD (2008) Reduced expression of Kir6.2/SUR2A subunits explains K_{ATP} deficiency in K^+ depleted rats. *Neuromuscul Disord* **18**:74–80.

von der Weid PY (1998) ATP-sensitive K^+ channels in smooth muscle cells of guinea-pig mesenteric lymphatics: role in nitric oxide and β -adrenoceptor agonist-induced hyperpolarizations. *Br J Pharmacol* **125**:17–22.

Weir MR (2003) Incidence of pedal edema formation with dihydropyridine calcium channel clockers: issues and practical significance. *J Clin Hypertens* **5**:330–335.

Welters A, Lerch C, Kummer S, Marquard J, Salgin B, Mayatepek E, and Meissner T (2015) Long-term medical treatment in congenital hyperinsulinism: a descriptive analysis in a large cohort of patients from different clinical centers. *Orphanet J Rare Dis* **10**:1-10.

Wickenden AD, Grimwood S, Grant TL, and Todd MH (1991) Comparison of the effects of the K^+-channel openers cromakalim and minoxidil sulphate on vascular smooth muscle. *Br J Pharmacol* **103**:1148–1152.

Wu SN, Wu AZ, Sung RJ (2007) Identification of two types of ATP-sensitive K^+ channels in rat ventricular myocytes*. Life Sciences* 80:378-387.

Zarghi A, Shafaati A, Foroutan SM, and Khoddam A (2004) Rapid determination of minoxidil in human plasma using ion-pair HPLC. *J Pharm Biomed Anal* **36**:377–379.

Downloaded from jpet.aspetjournals.org at ASPET Journals on April 18, 2024

JPET Fast Forward. Published on October 25, 2020 as DOI: 10.1124/jpet.120.000121
This article has not been copyedited and formatted. The final version may differ from this version.

Zarzoso M, Reiser M, and Noujaim SF (2018) *Cardiac Electrophysiology: From Cell to Bedside,* 7th ed. Philadelphia, Pennsylvania. eBook ISBN: 9780323448321.

Footnotes

a) **Financial Support:** This work was supported by the National Institutes of Health National Cancer Institute [R21CA131164]; the National Heart, Lung, and Blood Institute [R01HL146713]; the Systems Pharmacology and Toxicology Training Program [T32GM106999]; the Center for Studies of Host Response to Cancer Therapy through Center of Biomedical Research Excellence Award [P20GM109005], and the Center for Microbial Pathogenesis and Host Inflammatory Responses grant [P20GM103625] through the NIH National Institute of General Medical Sciences Centers of Biomedical Research Excellence. The content is solely the responsibility of the authors and does not necessarily represent the official views of the NIH.

b) This work has been partially presented in meeting abstracts:

Garner BR, Stolarz AJ, Fletcher TW, Rusch NJ. ATP-Sensitive K^+ Channels in Smooth Muscle Cells from Rat Mesenteric Lymph Vessels. *Poster presentation at Experimental Biology, Chicago, Illinois, April 2017.*

Garner BR, Stolarz AJ, Fletcher TW, Mu S, Rusch NJ. Potassium Channel Openers Inhibit Rhythmic Contractions and Lymph Flow in Rat Mesenteric Lymph Vessels. *Poster presentation at North American Vascular Biology Organization's Vasculata Workshop, St. Louis, Missouri, July 2018.*

c) Reprint requests should be directed to: Dr. Shengyu Mu (smu@uams.edu)

d) Author Affiliations

[1] Department of Pharmacology & Toxicology, College of Medicine, University of Arkansas for Medical Sciences, Little Rock, AR 72205

[2] Department of Pharmaceutical Sciences, College of Pharmacy, University of Arkansas for Medical Sciences, Little Rock, AR 72205

Downloaded from jpet.aspetjournals.org at ASPET Journals on April 18, 2024

JPET Fast Forward. Published on October 25, 2020 as DOI: 10.1124/jpet.120.000121
This article has not been copyedited and formatted. The final version may differ from this version.

[3] Arkansas Nanomedicine Center, College of Medicine, University of Arkansas for Medical Sciences, Little Rock, AR 72205

Figure Legends

Figure 1. Effect of cromakalim on the contractile behavior of isolated rat mesenteric LVs. A: Increasing concentrations of cromakalim (0.01 to 3 µmol/L, quarter-log increments) progressively inhibit the rhythmic contractions of isolated mesenteric LVs, ultimately leading to cessation of contractions. **B:** No significant changes in LV contractile parameters occurred with increasing concentrations of the DMSO solvent. Images in this figure are representative of n = 6 determinations.

Figure 2. Effect of clinically available KCOs on the contractile behavior of isolated rat mesenteric LVs. A: Increasing concentrations of minoxidil sulfate (0.01 to 100 µmol/L, half-log increments) progressively inhibited the rhythmic contractions of isolated mesenteric LVs, ultimately stopping contractions. **B:** Increasing concentrations of diazoxide (0.01 to 100 µmol/L, half-log increments) progressively inhibited the rhythmic contractions of isolated mesenteric LVs, but at higher concentrations than minoxidil sulfate. Images in this figure are representative of n = 6 determinations.

Figure 3. Profile of KCO effects on rhythmic contractions and intraluminal flow of isolated mesenteric LVs. Increasing concentrations of KCOs: cromakalim (**O**), minoxidil sulfate (■), and diazoxide (Δ) significantly decreased the amplitude of contraction **(A)**; progressively reduced the frequency of contraction **(B)**; resulted in a small but significant increase in end diastolic diameter (EDD) **(C)**; and decreased calculated lymph flow **(D)**. Data are reported as Mean ± S.D. analyzed using One-

Downloaded from jpet.aspetjournals.org at ASPET Journals on April 18, 2024

JPET Fast Forward. Published on October 25, 2020 as DOI: 10.1124/jpet.120.000121
This article has not been copyedited and formatted. The final version may differ from this version.

way ANOVA with Holm-Sidak post-test, significance refers to ANOVA. (n = 6, ** p < 0.01, **** p < 0.0001).

Figure 4. Cromakalim and minoxidil sulfate decrease lymph flow *in vivo*. Bathing the mesentery with HEPES PSS (□) did not significantly affect lymph flow, although there was a trend of increasing lymph flow during the experiment. Increasing concentrations of cromakalim (■) and minoxidil sulfate (■) significantly decreased lymph flow compared to HEPES PSS controls. Data reported as Mean ± S.D. analyzed using One-way ANOVA with Holm-Sidak post-test (n = 5, * p < 0.01, **** p < 0.0001). Significance reported over bars indicates significance compared to baseline. Significance denoted with labels indicates one-way ANOVA significance.

Figure 5. Expression of K_{ATP} channel subunits in LMCs. A: Mesenteric LVs were digested and co-incubated with a smooth muscle protein marker, α-smooth muscle actin-FITC (α –SMA-FITC). A gate was set around the cells staining positive for α-SMA. This gate is used in all subsequent panels. **B:** Cells selected from the α-SMA positive gate were co-incubated with Alexa-647 conjugated secondary antibody only as a negative control. **C:** α-SMA positive gated cells show immunoreactivity corresponding to Kir6.1. **D:** α-SMA positive-gated cells also exhibited Kir6.2 immunoreactivity. **E:** Immunoreactivity corresponding to SUR1 protein was not detected in α-SMA positive gated cells. **F:** α-SMA positive gated cells display immunoreactivity for SUR2. FSC, Forward Scatter. SSC, Side Scatter. Images in this figure are representative of n = 3 determinations.

Figure 6. ImageStream shows co-staining corresponding to the pore-forming Kir6.1 and Kir6.2 subunits on the LMC surface. In a single LMC, from left to right: Differential interference contrast (DIC) image shows single LMC morphology. α-SMA-FITC positive staining indicates the cell is a SMC. Kir6.1-Alexa647 blue fluorescence indicates surface expression of Kir6.1, whereas Kir6.2-Cy3 red fluorescence indicates the surface presence of Kir6.2. Images in this figure are representative of n = 50 images.

Downloaded from jpet.aspetjournals.org at ASPET Journals on April 18, 2024

JPET Fast Forward. Published on October 25, 2020 as DOI: 10.1124/jpet.120.000121
This article has not been copyedited and formatted. The final version may differ from this version.

Figure 7. Patch recordings of cromakalim-elicited K^+ currents. A: Cell-attached recording fails to reveal unitary K^+ currents at a patch potential of -50 mV. **B:** The same recording as in ***A*** after addition of 1 μmol/L cromakalim reveals channel activity. **C:** A plot of single-channel current amplitude as a function of patch potential depicts an average unitary conductance of 46.4 pS at negative patch potentials between -70 mV and -30 mV. Mild inward rectification results in a unitary conductance of 33.6 pS at positive patch potentials (+20 mV to +50 mV). Filled ovals located at the left of each trace represent the closed state. Data are reported as Mean ± S.D. (X,X) = (# cells, # of cell isolations from different animals).

Figure 8. Cell-attached recordings of K^+ currents elicited by minoxidil sulfate and diazoxide. Patch potential was maintained at -50 mV. Recordings failed to reveal unitary K^+ currents before (**A**) or after (**B**) addition of DMSO solvent. In another LMC initially exposed to control solution (**C**), the addition of 0.1 μmol/L minoxidil sulfate elicited unitary K^+ currents (**D**). Similarly, recordings in control solution were quiescent (**E**), whereas the addition of 3 μmol/L diazoxide elicited a current of similar amplitude as minoxidil sulfate (**F**).

Table 1. Measurements of contraction amplitude, contraction frequency, end diastolic diameter and intraluminal flow in isolated rat mesenteric lymph vessels in response to three different KCOs. Exposure of LVs to either increasing quarter-log concentrations of cromakalim (0.01-3 μmol/L), half-log concentrations of minoxidil sulfate, or half-log concentrations of diazoxide (0.01-100 μmol/L) progressively increased end diastolic diameter (EDD) concurrent with decreases in contraction frequency, amplitude, and calculated flow (* $p < 0.05$, ** $p < 0.01$, *** $p < 0.001$, **** $p < 0.0001$, Mean ± S.D., n = 6).

Downloaded from jpet.aspetjournals.org at ASPET Journals on April 18, 2024

JPET Fast Forward. Published on October 25, 2020 as DOI: 10.1124/jpet.120.000121
This article has not been copyedited and formatted. The final version may differ from this version.

KCO	Concentration (µmol/L)	Amplitude (% baseline)	Frequency (% baseline)	End Diastolic Diameter (% baseline)	Flow (% baseline)
Cromakalim	0.01	98.2 ± 5.4	102.1 ± 5.6	99.3 ± 0.9	99.5 ± 2.0
	0.0178	100.6 ± 5.6	96.4 ± 8.1	99.2 ± 1.3	95.5 ± 4.6
	0.03	98.5 ± 5.7	96.4 ± 9.8	98.9 ± 1.3	93.7 ± 9.2
	0.056	98.4 ± 6.2	97.5 ± 12.2	98.2 ± 1.6	93.8 ± 9.4
	0.1	98.0 ± 9.4	86.9 ± 16.0	98.7 ± 1.4	83.2 ± 11.6
	0.178	100.1 ± 16.2	58.8 ± 28.0 ****	100.4 ± 2.3	57.7 ± 26.7 ****
	0.3	68.1 ± 53.3	39.4 ± 32.1 ****	102.3 ± 3.4	40.2 ± 32.6 ****
	0.56	81.7 ± 41.2	27.4 ± 19.7 ****	103.2 ± 3.1	28.3 ± 20.9 ****
	1	33.2 ± 52.9 ***	4.4 ± 7.2 ****	105.3 ± 3.0 ***	4.5 ± 7.1 ****
	1.78	0.0 ± 0.0 ****	0.0 ± 0.0 ****	106.4 ± 3.5 ****	0.0 ± 0.0 ****
	3	0.0 ± 0.0 ****	0.0 ± 0.0 ****	106.9 ± 3.7 ****	0.0 ± 0.0 ****
Minoxidil Sulfate	0.01	100.0 ± 2.3	96.2 ± 7.2	100.2 ± 0.5	96.5 ± 7.5
	0.03	95.7 ± 11.6	90.9 ± 19.0	100.0 ± 1.8	86.9 ± 18.2

Downloaded from jpet.aspetjournals.org at ASPET Journals on April 18, 2024

JPET Fast Forward. Published on October 25, 2020 as DOI: 10.1124/jpet.120.000121
This article has not been copyedited and formatted. The final version may differ from this version.

	0.1	96.0 ± 14.7	84.3 ± 23.2	100.3 ± 1.6	80.7 ± 22.4 *
	0.3	95.8 ± 19.7	56.9 ± 24.6 ****	101.6 ± 1.5	55.6 ± 26.2 ****
	1	56.1 ± 49.1 **	18.6 ± 21.8 ****	102.3 ± 1.4	17.9 ± 21.5 ****
	3	49.5 ± 54.4 **	4.0 ± 4.6 ****	103.2 ± 1.9 **	4.1 ± 4.6 ****
	10	0.0 ± 0.0 ****	0.0 ± 0.0 ****	103.7 ± 1.7 **	0.0 ± 0.0 ****
	30	0.0 ± 0.0 ****	0.0 ± 0.0 ****	103.9 ± 1.9 ***	0.0 ± 0.0 ****
	100	0.0 ± 0.0 ****	0.0 ± 0.0 ****	104.3 ± 1.8 ***	0.0 ± 0.0 ****
Diazoxide	0.01	99.1 ± 6.5	99.4 ± 9.0	99.8 ± 0.9	98.4 ± 5.3
	0.03	102.4 ± 10.9	95.0 ± 11.5	99.9 ± 1.2	96.3 ± 6.2
	0.1	101.7 ± 10.8	96.6 ± 10.5	99.6 ± 0.8	97.1 ± 5.8
	0.3	101.2 ± 11.6	93.8 ± 14.3	99.6 ± 0.7	93.8 ± 11.1
	1	100.0 ± 12.2	89.7 ± 8.3	100.3 ± 1.3	89.9 ± 7.3
	3	100.2 ± 10.2	82.6 ± 10.6 *	101.3 ± 2.2	83.9 ± 8.6 *
	10	101.3 ± 9.1	45.5 ± 19.5 ****	102.4 ± 6.5	47.1 ± 18.2 ****
	30	52.1 ± 57.5 ****	10.5 ± 17.4 ****	104.6 ± 7.4	10.2 ± 16.5 ****

Downloaded from jpet.aspetjournals.org at ASPET Journals on April 18, 2024

JPET Fast Forward. Published on October 25, 2020 as DOI: 10.1124/jpet.120.000121
This article has not been copyedited and formatted. The final version may differ from this version.

	100	0.0 ± 0.0 ****	0.0 ± 0.0 ****	106.3 ± 7.1 *	0.0 ± 0.0 ****

Table 2. Topical superfusion of cromakalim or minoxidil sulfate decreased volumetric lymph flow in rat mesenteric LVs in vivo. Increasing log-concentrations of cromakalim or minoxidil sulfate (0.01-10 μmol/L) progressively decreased positive volumetric lymph flow compared to the DMSO solvent control (* $p < 0.05$, Mean ± S.D., $n = 5$).

KCO	Concentration (μmol/L)	Positive Volumetric Flow (% baseline)
Cromakalim	0.01	121.2 ± 42.4
	0.1	50.6 ± 22.0 *
	1	48.6 ± 23.3 *
Minoxidil Sulfate	0.01	99.7 ± 29.8
	0.1	85.6 ± 13.6

Downloaded from jpet.aspetjournals.org at ASPET Journals on April 18, 2024

JPET Fast Forward. Published on October 25, 2020 as DOI: 10.1124/jpet.120.000121
This article has not been copyedited and formatted. The final version may differ from this version.

	1	46.4 ± 6.3 *
DMSO	2.82	121.2 ± 49.2
	28.16	121.9 ± 55.9
	281.58	136.0 ± 65.8

Downloaded from jpet.aspetjournals.org at ASPET Journals on April 18, 2024

Table 3. Cycle thresholds for real-time PCR amplification using TaqMan™ primers specific for K_{ATP} channel subunits in whole rat mesenteric LVs. Transcripts encoding all four known K_{ATP} channel subunits were detected, including the pore-forming Kir6.1 and Kir6.2 subunits, and the regulatory SUR1 and SUR2 subunits. However, the SUR1 transcript was extremely sparse. GAPDH was the amplification standard. Data reported as Mean ± S.D., n = 3.

Channel Subunits	**Cycle Thresholds**
Kir6.1	25.9 ± 1.6
Kir6.2	24.0 ± 1.6

JPET Fast Forward. Published on October 25, 2020 as DOI: 10.1124/jpet.120.000121
This article has not been copyedited and formatted. The final version may differ from this version.

SUR1	31.6 ± 1.3
SUR2	25.3 ± 1.7
GAPDH	25.7 ± 3.0

Downloaded from jpet.aspetjournals.org at ASPET Journals on April 18, 2024

JPET Fast Forward. Published on October 25, 2020 as DOI: 10.1124/jpet.120.000121
This article has not been copyedited and formatted. The final version may differ from this version.

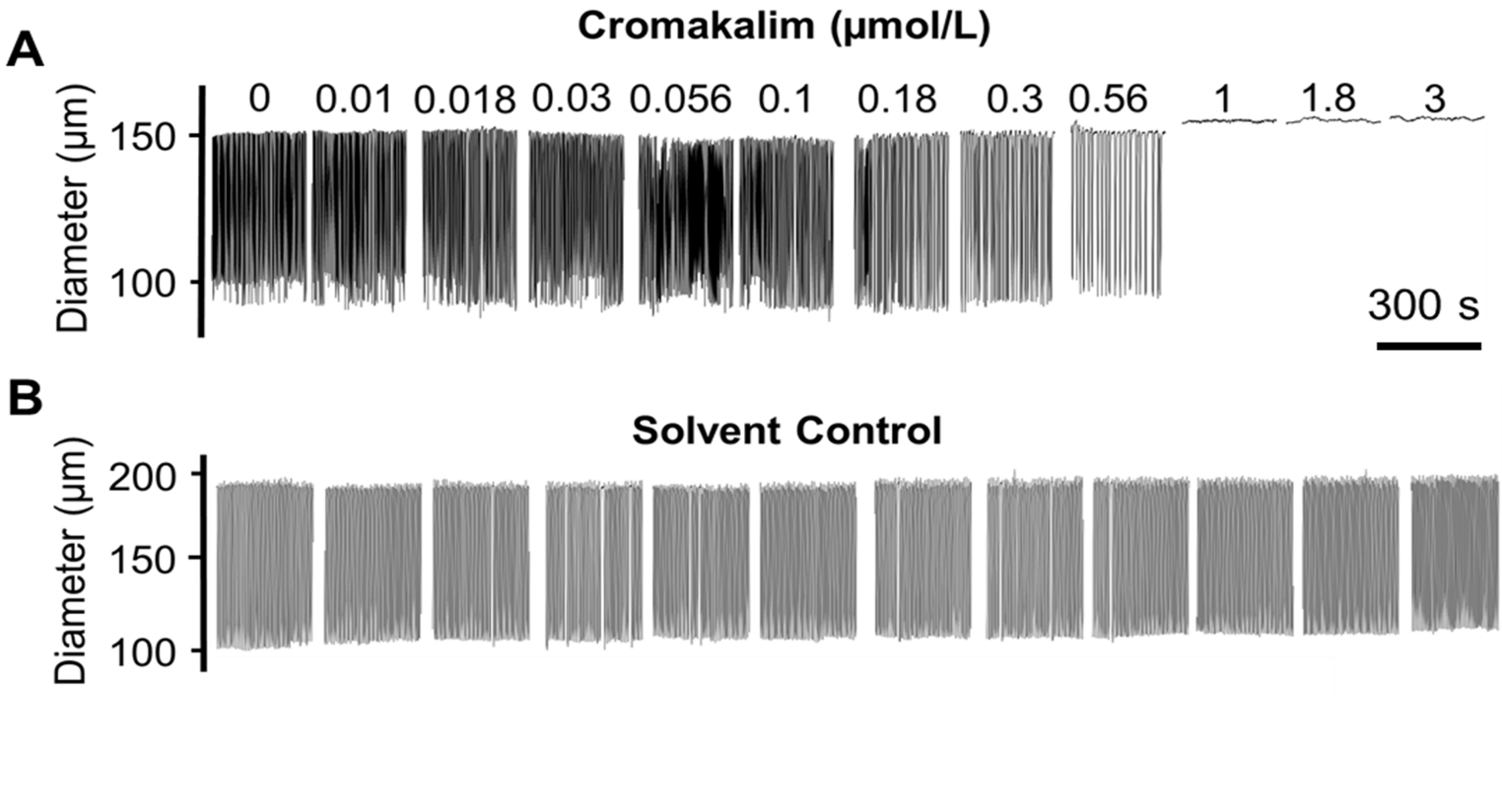

Figure 1

Downloaded from jpet.aspetjournals.org at ASPET Journals on April 18, 2024

JPET Fast Forward. Published on October 25, 2020 as DOI: 10.1124/jpet.120.000121
This article has not been copyedited and formatted. The final version may differ from this version.

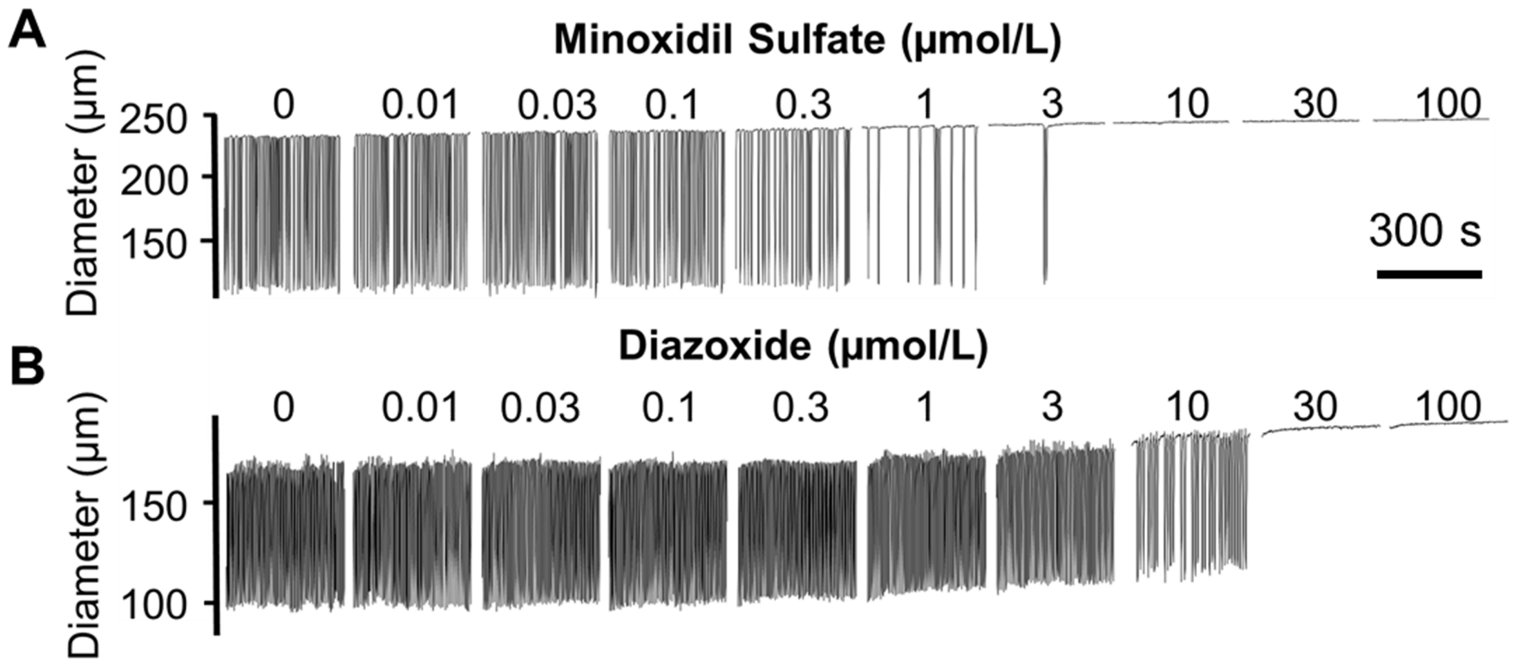

Figure 2

Downloaded from jpet.aspetjournals.org at ASPET Journals on April 18, 2024

JPET Fast Forward. Published on October 25, 2020 as DOI: 10.1124/jpet.120.000121
This article has not been copyedited and formatted. The final version may differ from this version.

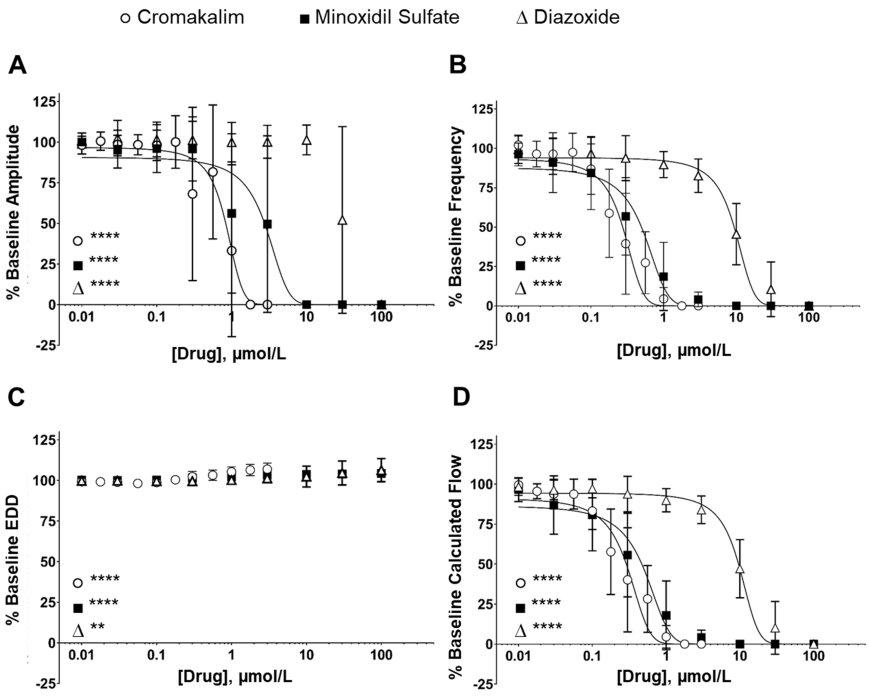

Figure 3

Downloaded from jpet.aspetjournals.org at ASPET Journals on April 18, 2024

JPET Fast Forward. Published on October 25, 2020 as DOI: 10.1124/jpet.120.000121
This article has not been copyedited and formatted. The final version may differ from this version.

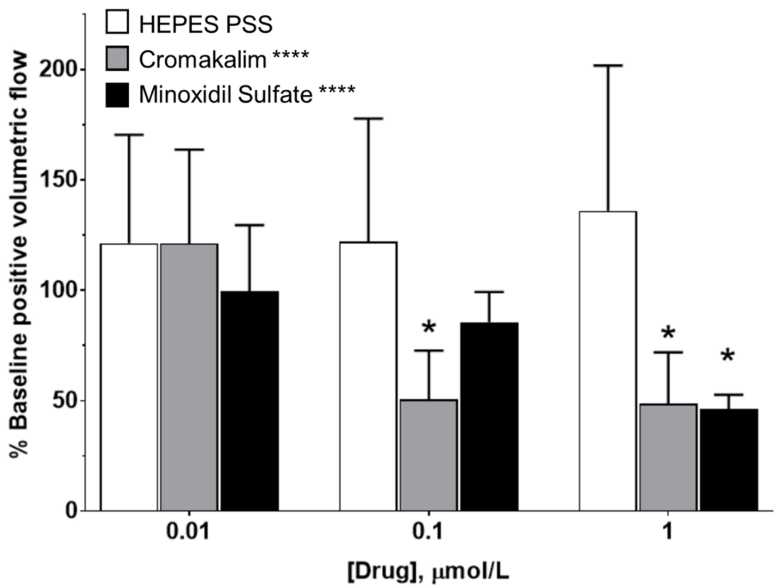

Figure 4

Downloaded from jpet.aspetjournals.org at ASPET Journals on April 18, 2024

JPET Fast Forward. Published on October 25, 2020 as DOI: 10.1124/jpet.120.000121
This article has not been copyedited and formatted. The final version may differ from this version.

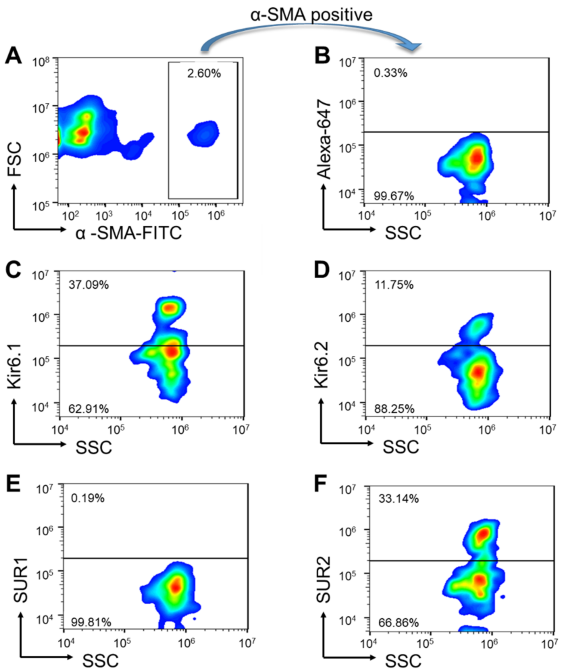

Figure 5

Downloaded from jpet.aspetjournals.org at ASPET Journals on April 18, 2024

JPET Fast Forward. Published on October 25, 2020 as DOI: 10.1124/jpet.120.000121
This article has not been copyedited and formatted. The final version may differ from this version.

Figure 6

Downloaded from jpet.aspetjournals.org at ASPET Journals on April 18, 2024

JPET Fast Forward. Published on October 25, 2020 as DOI: 10.1124/jpet.120.000121
This article has not been copyedited and formatted. The final version may differ from this version.

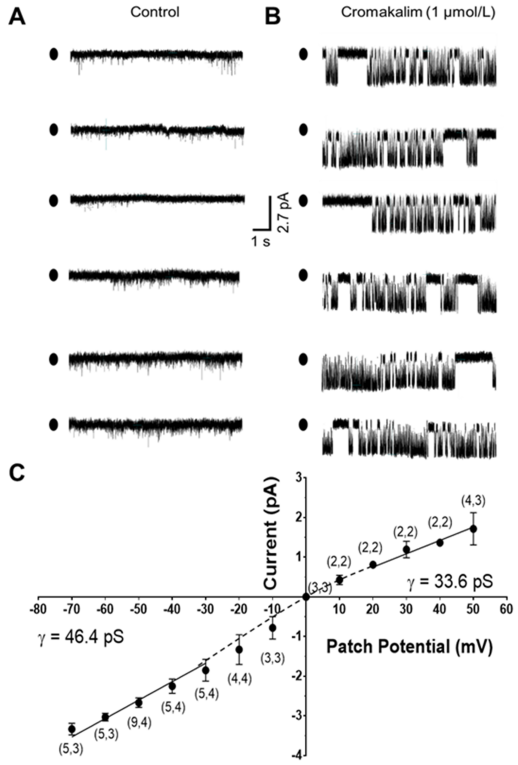

Figure 7

Downloaded from jpet.aspetjournals.org at ASPET Journals on April 18, 2024

JPET Fast Forward. Published on October 25, 2020 as DOI: 10.1124/jpet.120.000121
This article has not been copyedited and formatted. The final version may differ from this version.

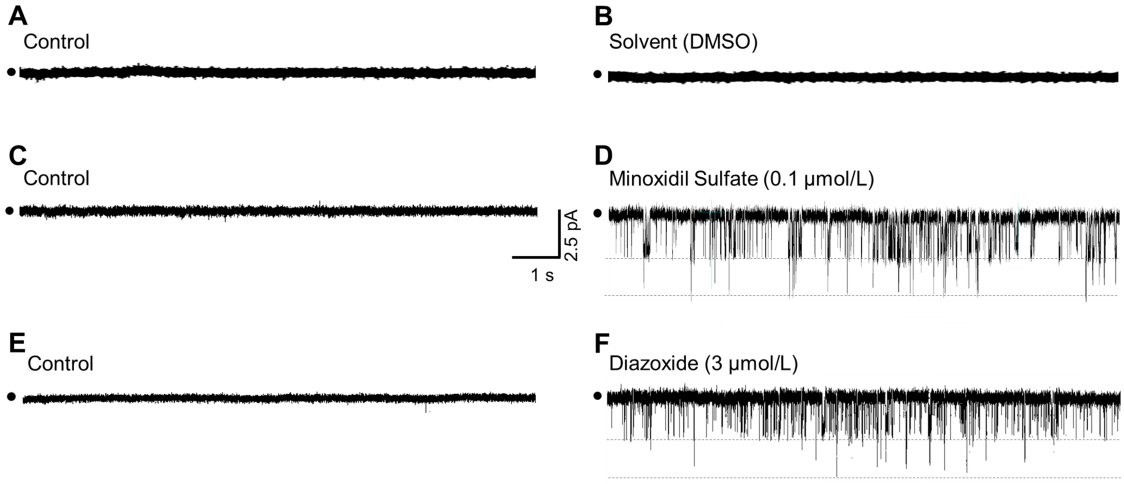

Figure 8

Downloaded from jpet.aspetjournals.org at ASPET Journals on April 18, 2024

K_{ATP} Channel Openers Inhibit Lymphatic Contractions and Lymph Flow as a Possible Mechanism of Peripheral Edema

Brittney R. Garner, Amanda J. Stolarz, Daniel Stuckey, Mustafa Sarimollaoglu,

Yunmeng Liu, Philip T. Palade, Nancy J. Rusch, and Shengyu Mu

Journal of Pharmacology and Experimental Therapeutics

Supplemental Data

Supplemental Table 1. TaqMan™ primers were used to amplify cDNA corresponding to K_{ATP} channel subunits in whole rat mesenteric lymph vessels. These subunits included the pore-forming Kir6.1 and Kir6.2 subunits, and ancillary SUR1 and SUR2 subunits. Subsequently, primary antibodies targeting the same K_{ATP} channel subunits were used to immunostain single rat mesenteric LMCs for use in flow cytometry or ImageStream® assays.

Primers			
Subunit	**Gene**	**GenBank Accession Number**	**Lot Number**
Kir6.1	Kcnj8	NM_017009.4	P170412-003 B09
Kir6.2	Kcnj11	NM_031358.3	P170416-001 B03
SUR1	Abcc8	NM_013039.2	P170420-000 B06
SUR2	Abcc9	NM_013040.2	P170412-003 B11

Antibodies					
Subunit	**Host Species**	**Company**	**Catalog**	**Epitope**	**Concentration**
Kir6.1	Rabbit	Alomone	#APC-105	aa 382-396	1:50
Kir6.2	Rabbit	Alomone	#APC-020	aa 372-385	1:50
Kir6.2	Guinea Pig	Alomone	#AGP-067	aa 372-385	1:50

SUR1	Rabbit	Abcam	ab32844	aa 1560-1582	1:50
SUR2	Rabbit	Abcam	ab84299	aa 1440-1489	1:50

Supplemental Table 2. Increasing concentrations of DMSO did not significantly affect rhythmic contractions in isolated rat mesenteric lymph vessels (LVs). Exposure of LVs to cumulative concentrations of DMSO (2.82 µmol/L to 720.85 µmol/L) had no significant effect on contraction amplitude and frequency, end diastolic diameter or calculated lymph flow compared to baseline values. Data reported as Mean ± S.D., n = 5.

	Concentration (µmol/L)	Amplitude (% baseline)	Frequency (% baseline)	End Diastolic Diameter (% baseline)	Flow (% baseline)
DMSO	2.8	100.8 ± 4.0	103.1 ± 9.6	99.9 ± 0.7	105.4 ± 7.4
	5.0	98.5 ± 5.1	100.6 ± 12.8	99.5 ± 1.4	100.8 ± 8.1
	5.6	106.2 ± 13.8	99.3 ± 14.2	98.9 ± 1.6	104.7 ± 20.4
	10.8	98.9 ± 4.7	104.6 ± 19.0	98.2 ± 3.2	102.3 ± 11.8
	19.7	97.8 ± 5.4	107.5 ± 23.3	98.6 ± 2.8	106.0 ± 17.9
	50.1	98.1 ± 4.8	108.6 ± 31.9	98.6 ± 3.1	107.2 ± 25.5
	72.1	96.1 ± 5.8	113.2 ± 38.7	98.2 ± 4.0	109.4 ± 33.0
	107.6	94.6 ± 7.8	107.5 ± 34.0	97.5 ± 5.2	103.0 ± 34.9
	197.1	89.2 ± 14.3	117.5 ± 38.0	97.8 ± 6.0	104.3 ± 43.8
	501.2	92.1 ± 7.7	119.4 ± 43.5	100.8 ± 1.2	113.5 ± 46.1

	720.8	91.8 ± 9.3	118.4 ± 47.7	100.7 ± 2.1	112.5 ± 52.7

Supplemental Figure 1. Glibenclamide partially prevents cromakalim-induced attenuation of rhythmic contractions in isolated rat mesenteric lymph vessels. A, B: Cumulative concentrations of cromakalim (○) reduced the amplitude and frequency of rhythmic contractions, respectively, and preincubation with 1 μmol/L glibenclamide (●) significantly attenuated this effect. **C:** Glibenclamide did not affect cromakalim-induced increases in end diastolic diameter (EDD), but **D:** partially prevented cromakalim-induced reductions in calculated lymph flow. Data reported as Mean ± S.D., n = 5. Significance denoted by unpaired one-tailed t test, comparing IC_{50} values. *** $p < 0.001$, **** $p < 0.0001$.